Development of empirical models for an estate level air temperature prediction in Singapore

Steve Kardinal Jusuf* and Wong Nyuk Hien, National University of Singapore, Singapore,
****Corresponding author email: stevekj@nus.edu.sg***

ABSTRACT

Urban heat island (UHI) phenomenon has become a common problem in many major cities worldwide including Singapore. As a small island state, it is very important for Singapore to carefully plan its urban development. However, urban planners have no assessment tool to evaluate their planning impacts on the environment, especially the impact on air temperature due to the change of land use. This paper discusses the development of an empirical model for air temperature prediction to evaluate the impact of estate development by means of Geographical Information System (GIS).

Empirical models of minimum (T_{min}), average (T_{avg}) and maximum (T_{max}) air temperature for Singapore estate have been developed and validated, based on the long-term field measurement between the period of September 2005 and March 2008. The independent variables that were used in the models are *daily minimum (Ref T_{min}), average (Ref T_{avg}) and maximum (Ref T_{max}) temperature* at reference point, *average of daily solar radiation* (SOLAR), *percentage of pavement area over R 50m surface* area (PAVE), *average height to building area ratio* (HBDG), *total wall surface area* (WALL), *Green Plot Ratio* (GnPR), *sky view factor* (SVF) and average surface albedo (ALB).

Sensitivity analyses were carried out to observe the dependence of the air temperature due to the variations of each variable. An ideal type of urban canyon was used to simplify the variation of building, pavement and greenery distributions. The sensitivity analyses were carried out by varying some of the following important parameters: the *greenery density* (GnPR), which may affect the SVF; the *building height*, which affects the SVF, WALL and HBDG values; and *canyon width*, which affects the SVF, PAVE AND HBDG values.

The Screening Tool for Estate Environment Evaluation (STEVE) was developed with the motivation to bridge between research findings, especially the air temperature prediction models and the urban planners.

Introduction

Urban development is imperative for economic growth and national development. Differential over development of cities as compared to neighborhood towns and villages attracts more inhabitants to cities leading to an aggravated need to further develop the cities. According to Laski and Schellekens (2007), in 2008, more than half of the world population is living in urban areas and the numbers are estimated to grow up to 5 billion people by 2030.

The problem of urbanization is not an exception to Singapore. Urbanization in this city-state extends beyond its border to its neighboring countries and even to its regional South East Asian countries. Known as the politically stable and the safest country in Asia, Singapore attracts a large pool of foreign talent and traders from all over the world. Furthermore, the government has a plan to increase the population to 6.5 million in 40-50 years from the current 4.5 million (AP, 2007). New urban developments can be expected to accommodate the social and economical needs of people. With the current inhabitants and limited land area of 707.1 km^2, Singapore has already become the second most densely

populated independent country in the world excluding Macau (see: Wikipedia, 2008). Without careful urban planning that incorporates environmental sustainability, adverse impacts on urban climate condition may emerge, such as urban heat island (UHI), thermal discomfort and pollutions. The detail of Singapore urban planning concept has actually been described in the 2001 Concept Plan. However, by far, environmental impact assessment is not a mandatory requirement in the Singapore urban development. Furthermore, urban planners have no assessment tool and method to evaluate their planning impacts on the environment.

Closely related to the urbanization, UHI phenomenon has become a common problem in many major cities worldwide (Oke 1971; Padmanabhamurty, 1990/91; Sani 1990/91; Swaid and Hoffman, 1990; Eliasson, 1996; Giridharan, *et.al.*, 2007) as well as in Singapore (Wong and Chen, 2009). This phenomenon is mainly due to the loss of greenery area for the purpose of urban development.

This paper discusses the development of an empirical model for air temperature prediction to evaluate the impact of estate development by means of Geographical Information System (GIS).

Background study (Wong, *et.al.*, 2007; Jusuf, *et.al.* 2007; Wong and Jusuf, *submitted*) was conducted to investigate the existence of temperature patterns in relation with the urban morphology conditions, which is important to develop the air temperature prediction models. The study concluded the existence of temperature pattern that is closely related to the urban land use. It was found that during daytime, the industrial area exhibits a higher surface temperature than commercial and business areas, and park area has the lowest surface temperature. However, at night, on the contrary, the commercial and business areas exhibit a higher ambient temperature compared with industrial and airport areas. The industrial areas consist of low building height, large pavement area, less vegetations and light roof structures, which have less shading and extensive use of heat absorbing building materials. As a result, it has high temperature during daytime. On the other hand, it is cool during nighttime, since the heat stored during daytime is easily released to sky with less obstruction from the surrounding buildings. This temperature pattern preliminary indicates its relationship with the surrounding distribution of greenery, building and pavement.

Hence, the hypothesis of urban air temperature are proposed as: "the air temperature of a point at a certain height level is the function of the local climate characteristics, which deviates according to the surrounding urban morphology characteristics (building, pavement and greenery) at a ***certain radius***".

Methodology

Air temperature prediction models

The field measurements data for the models development were between September 2005 and March 2008. Meanwhile, field measurement data between April and June 2008 was used for model validation. Table 1 shows the overall period of measurements in NUS and One-North.

HOBO data loggers together with solar covers were used in the measurements. They were attached to the lampposts in various locations in NUS and One-North; and configured at 10-minutes interval throughout the measurement periods. The air temperature data was obtained by sampling at a height of 1.8 m for each of the location as shown in Figure 1. The sensors were factory calibrated.

As a reference point, meteorological data was gathered from nearby station, which maintained by National University of Singapore (Department of Geography, 2008). The data

analysis focuses on fairly clear, calm (wind speed <3m/s) and hot weather condition, selected by analyzing the solar radiation, wind speed and air temperature data of the reference point.

Table 1. Overall periods of measurements in NUS and One-North

ESTATE	TYPE OF MEASUREMENT	PERIOD OF MEASUREMENT
NUS	Estate-wide	10th-24th September 2005
NUS	Estate-wide	26th August-25th September 2006
NUS	Canyon (ENG & PGP)*	17th July-20th October 2007
NUS	Canyon (PGP, SD2 & SD4)*	23rd October 2007-31st March 2008
One-North	Estate-wide	23rd October 2007-31st March 2008
One-North	Canyon (AYER, BIO, ROCH)*	23rd October 2007-31st March 2008
One-North	Canyon (AYER, BIO, ROCH)* for model validation	1st April-30th June 2008

* Engineering (ENG), Price George's Park (PGP), Science Drive 2 (SD2), Science Drive 4 (SD4), Ayer Rajah Industrial Estate (AYER), Biopolis (BIO) and Rochester Park (ROCH)

Daily minimum (T_{min}), average (T_{avg}) and maximum (T_{max}) temperature of each point of measurements were calculated as dependent variable of the air temperature prediction model. The independent variables of the models can be categorized into:

1. Climate predictors: *daily minimum (Ref T_{min}), average (Ref T_{avg}) and maximum (Ref T_{max}) temperature* at reference point; *average of daily solar radiation* (SOLAR). For the SOLAR predictor, average of daily solar radiation total ($SOLAR_{total}$) was used in T_{avg} models, while average of solar radiation maximum of the day ($SOLAR_{max}$) was used in the T_{max} model. SOLAR predictor is not applicable for T_{min} model.
2. Urban morphology predictors: *percentage of pavement area over R 50m surface* area (PAVE), *average height to building area ratio* (HBDG), *total wall surface area* (WALL), *Green Plot Ratio* (GnPR), *sky view factor* (SVF) and average surface albedo (ALB).

Wind speed, one of the most common variables, was excluded in the model development, since the models focus on calm day conditions. Meanwhile for another common variable, altitude, Kestrel 4200 pocket weather tracker was used to measure the altitude of each measurement point. The measurement results show that the altitude difference across the two estates is only about 56m, which is considered as relatively flat. The highest location is 156m above sea level at Point 1, NUS estate and the lowest point is 98m above sea level at Rochester Park, One-North. The 56m altitude difference will only influence the air temperature condition under ideal condition of about 0.36K, based on atmospheric lapse rate of -0.0065^{o}C/m (ISO, 1975). It means that altitude has a very little influence on air temperature condition. Hence, altitude is excluded from the model development.

In collecting the urban morphology predictors, master plan drawings of NUS and One-North obtained from the relevant agencies were used and inputted to GIS to quantify the PAVE and WALL areas. Field surveys had also been done to verify and update the drawings. Besides PAVE area, the building (BDG) and greenery (GREEN) areas were also quantified. BDG was calculated based on 2-D footprint area, while PAVE and GREEN areas were calculated in 3-D areas; following the contour of the land surfaces. BDG results were then used to calculate the HBDG variable, while GREEN was used to calculate GnPR variable. HBDG represents the thermal mass of the environment within the radius of influence area by calculating the ratio of average building heights over the total floor areas (Knowles, 1977; Giridharan, *et.al.*, 2008). WALL variable indicates the building density in the area.

Figure 1. Points of measurements on NUS (above) and One-North (below) sites

The ALB values were taken by field measurements. Two silicon pyranometers (one was directed to the sky and another one was directed to the wall) were used together with a data logger, simultaneously mounted on a lamppost and recorded the solar radiation for few days depending on the weather condition. Then, the pyranometers were moved and redirected to different locations to record the albedo of the surrounding environment.

SVF of each measurement point was measured by means of Nikon Digital camera and fish eye lens. The images were processed into black and white images, in which sky is white and building and trees are black. Then, the images were put into RayMan 1.2 software to calculate the SVF (Matzarakis, 2000).

Before the model was developed, the radius of influence area was determined. Giridharan, *et.al.*, (2007) used 15-17.5 m radius as the influence area to study the effect of greenery and it was found that 15-17.5 m radius was not able to explain the significant impact to the air temperature. Meanwhile, Kruger (2007) studied three different influence area radiuses of 56m, 125m and 565m and found that radius 56m has a more significant effect on the model's correlation coefficient.

In the preliminary study, there were four different radiuses of influence areas to be selected as the most significant. The radiuses were 25m, 50m, 75m and 100m, see Figure 2. BDG and PAVE areas were correlated with T_{min}, T_{avg} and T_{max} to provide indication of the radius of influence area. Table 2 shows that radius 50m and 75m are the top two radiuses, which have higher F and R^2 values, although 75m radius seems to have the highest ones. Further selection was done by including all of the mentioned variables and found that 50m radius has more significant influence areas than the other radiuses. Consequently, this chapter will analyze and discuss the air temperature prediction models based on 50m radius. This result agrees with the Kruger analysis (2007).

Figure 2. Sample of NUS measurement point in influence area radius of 25m, 50m, 75m and 100m

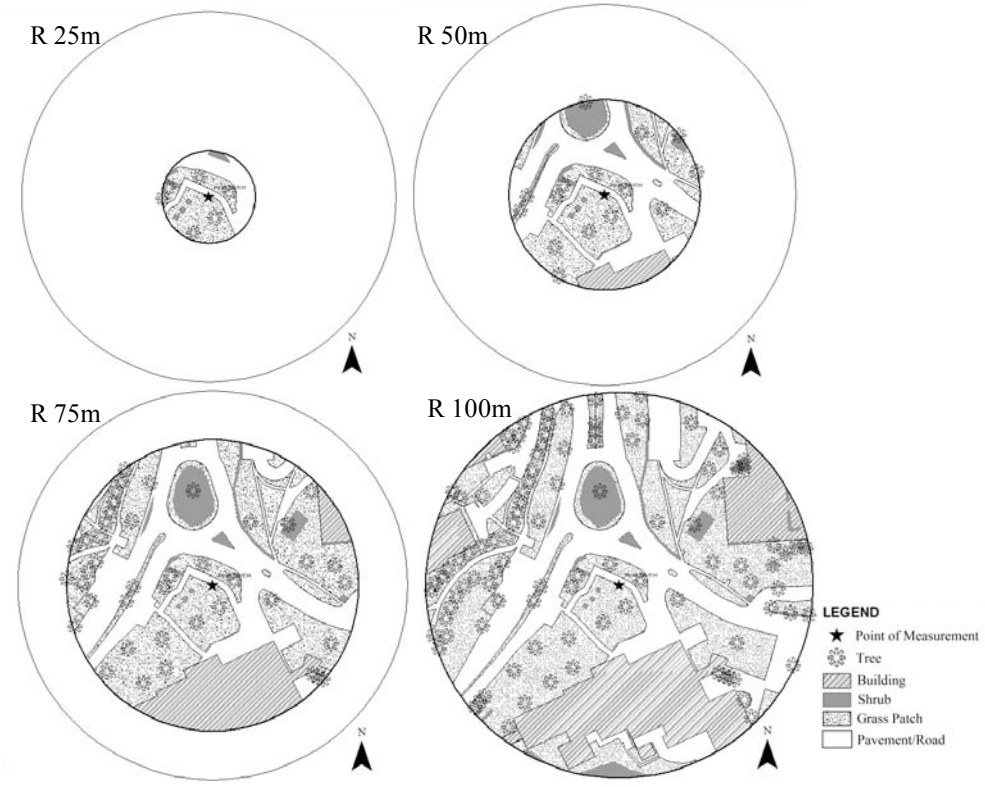

Table 2. Preliminary study on radius of influence area

RADIUS (m)	T_{min}			T_{avg}			T_{max}		
	R^2	F	Significance (p<0.05)	R^2	F	Significance (p<0.05)	R^2	F	Significance (p<0.05)
25	0.28	21.79	YES	0.22	15.13	YES	0.05	3.09	NO
50	0.32	25.84	YES	0.26	19.43	YES	0.10	5.76	YES
75	0.34	28.27	YES	0.29	22.51	YES	0.10	5.96	YES
100	0.31	24.62	YES	0.25	18.64	YES	0.08	4.83	YES

Sensitivity Analysis

The sensitivity analyses were carried out to analyze the dependence of the air temperature due to the variations of each variable. An ideal type of urban canyon (see Figure 3a) was used to simplify the variation of building, pavement and greenery distributions. Table 3 shows the climatic predictors values at the weather station that were used in this sensitivity analyses based on the conditions on 3rd November 2007 and Table 4 shows the variables modified in different temperature models for the sensitivity analyses.

Figure 3. Building layout model for sensitivity analysis (a) and Building layout model 3 on change of canyon width (b).

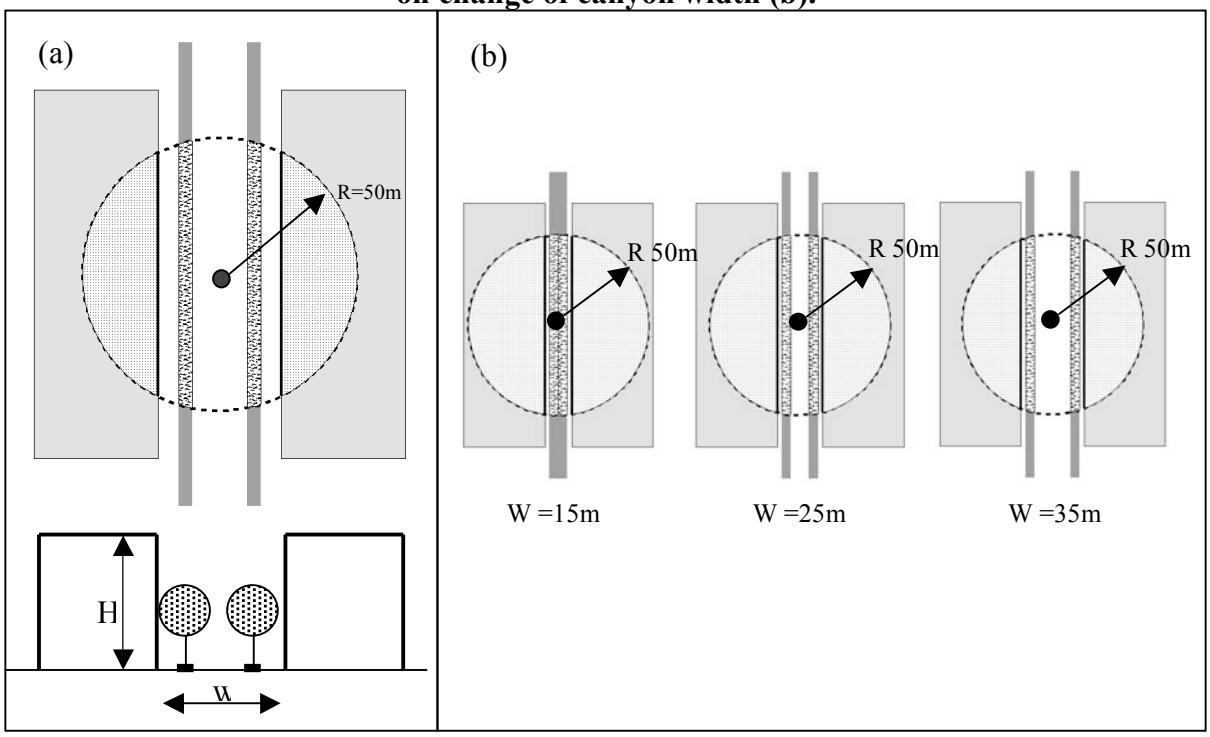

The analyses were done by varying some of the following important parameters: the *greenery density* (GnPR), which may affect the SVF; the *building height*, which affects the SVF, WALL and HBDG values; and *canyon width* (Figure 3b), which affects the SVF, PAVE AND HBDG values.

In relation to the above building layout models, given a fixed surface area of 50m radius, the change of GnPR depends on the species (LAI) and numbers of the plants, regardless the height of the plants (shrubs or trees). In these sensitivity analyses and models application studies, only the increase of GnPR due to the trees was considered, in which, the

trees will have impact on the reduction of SVF value. Therefore, it is necessary to derive an estimated value of how much reduction of SVF value due to the increase of 1 GnPR.

To derive the estimated SVF reduction value, 46 of the 110 measurement points were statistically analyzed (see Table 5). Mature trees predominantly influenced the GnPR of these 46 measurement points, which in turn, affected the SVF values. From the regression result, eqn. 1, it can be estimated that the SVF value reduces about 0.2 for every GnPR increase of 1.

$$SVF = 0.962 - 0.219\ GnPR$$
$$R^2 = 0.44 \text{ and } F = 35.17 (Sig.\ 0.00) \quad (1)$$

Table 3. Input on climate predictors based on data at weather station

Date	3 November 2007
Min. Temp. at reference point (Ref Tmin)	26.0 °C
Avg. Temp. at reference point (Ref Tavg)	27.7 °C
Max. Temp. at reference point (Ref Tmax)	30.6 °C
Total solar radiation ($SOLAR_{total}$)	3689.04 W/m^2
Max. solar radiation ($SOLAR_{max}$)	707 W/m^2

Table 4. Model scenarios for the sensitivity analyses

		Model 1	Model 2	Model 3
Variables to be modified		GnPR	No of storey, GnPR	Canyon Width, GnPR
Parameters	No of storeys (@ 4m)	4	1-60 (Even no)	4
	Canyon width	45m	45m	15m, 25m, 35m, 45m
	Greenery strips width	5m	5m	5m
	GnPR	0, 1, 2, 3, 4, 5, 6, 7, 8	0, 1, 2, 3, 4, 5, 6	0, 1, 2, 3, 4, 5, 6

Table 5. The selected 46 measurement points

ESTATE	POINT NAME	ESTATE	POINT NAME	ESTATE	POINT NAME	ESTATE	POINT NAME
NUS	POINT 1	NUS	POINT 17	One-North	POINT 10	One-North	POINT 28
NUS	POINT 2	NUS	POINT 18	One-North	POINT 11	One-North	POINT 30
NUS	POINT 3	NUS	POINT 21	One-North	POINT 12	One-North	BIO 1
NUS	POINT 5	NUS	POINT 22	One-North	POINT 13	One-North	ROCH 2
NUS	POINT 6	NUS	POINT 24	One-North	POINT 14	One-North	ROCH 3
NUS	POINT 8	NUS	POINT 25	One-North	POINT 15	One-North	ROCH 4
NUS	POINT 9	NUS	POINT 30	One-North	POINT 16	One-North	ROCH 5
NUS	POINT 10	One-North	POINT 1	One-North	POINT 17	One-North	ROCH 6
NUS	POINT 11	One-North	POINT 5	One-North	POINT 18	One-North	ROCH 7
NUS	POINT 12	One-North	POINT 7	One-North	POINT 19	One-North	ROCH 8
NUS	POINT 15	One-North	POINT 8	One-North	POINT 20	One-North	ROCH 9
NUS	POINT 16	One-North	POINT 9	One-North	POINT 27		

Results and Discussions

Air temperature prediction models

Models development. In the first stage of model development, trend analysis was done to identify and discuss the behavior of the models' variables, by examining the variables' regression coefficient values and their correlations with the dependent variable (Pearson Correlation). Not all of the independent variables are significant; however, it is important to analyze how these variables behave in determining the air temperature. Table 6 shows the regression results for T_{min}, T_{avg} and T_{max} models. The correlation coefficients for T_{min} and T_{avg} models are high at 0.86 and 0.92 respectively, while it is fair at 0.54 for T_{max} model.

SOLAR, PAVE, HBDG and WALL variables in all of the models are in line with the general theory of factors that influence the air temperature. Both signs, in regression and Pearson correlation are the same.

In general, extensive use of concrete and other heat absorbing surfaces (PAVE) increases urban air temperature by decreasing the surface moisture available for evapotranspiration. Furthermore, more solar radiation is absorbed and reradiated into heat because dry surfaces have low albedo (ALB) value (Santamouris, 2001).

Table 6. Regression results of air temperature prediction model

VARIABLES	T_{min} R 50M			VARIABLES	T_{avg} R 50M			VARIABLES	T_{max} R 50M		
	B	Sig.	Pearson Correlation		B	Sig.	Pearson Correlation		B	Sig.	Pearson Correlation
Constant	3.548			Constant	1.842	0.00		Constant	7.511		
Ref T_{min}	0.848	0.00	0.89	Ref T_{avg}	0.915	0.00	0.91	Ref T_{max}	0.684	0.00	0.50
$SOLAR_{total}$	NA	NA	NA	$SOLAR_{total}$	5.782E-05	0.00	0.50	$SOLAR_{max}$	0.0030	0.00	0.15
PAVE	0.003	0.00	0.27	PAVE	0.007	0.00	0.34	PAVE	0.006	0.00	0.24
GnPR	-0.159	0.00	-0.18	GnPR	-0.037	0.00	-0.23	GnPR	0.009	0.52	-0.28
HBDG	-0.030	0.00	-0.13	HBDG	-0.015	0.00	-0.08	HBDG	-0.016	0.00	-0.03
WALL	1.674E-05	0.00	0.40	WALL	1.539E-05	0.00	0.42	WALL	7.391E-06	0.00	0.19
SVF	0.113	0.07	-0.06	SVF	0.614	0.00	0.07	SVF	1.475	0.00	0.39
ALB	0.911	0.00	-0.09	ALB	0.991	0.00	-0.01	ALB	1.492	0.00	0.23
F	1240.77			*F*	1994.50			*F*	211.57		
R^2	0.86			R^2	0.92			R^2	0.54		
Std Error	0.47			Std Error	0.27			Std Error	0.59		

The thermal mass, HBDG and wall surface area, WALL, of each point are in line with the general theory. They have negative signs and positive signs respectively in both regression coefficient and Pearson correlation. The higher the thermal mass of the environment, the lower the temperature is, since it reduces the heat released to the surrounding environment. Meanwhile, large wall surface area leads to a higher air temperature, since the wall reflects short wave and long wave solar radiation to the environment.

Greenery is one of the important factors in Singapore's urban development. It shapes its pleasant urban environment. The regression models verify that greenery, noted as GnPR, provides a good impact to the environment. It reduces the air temperature, shown as negative values in both regression coefficient and Pearson correlation in the T_{min} and T_{avg} models. However, in the T_{max} model, GnPR shows positive and negative values in the regression coefficient and Pearson correlation respectively. It is believed that the existence of anthropogenic heat further increases air temperature and greenery effect becomes less significant.

The SVF variable has a positive sign in all of the models, which seems not in line with the general theory that low SVF leads to high nocturnal air temperature Oke, 1981; Oke, *et.al.*, 1991; Chapman, *et.al.*, 2001). A detail study has been done and discussed to investigate the correlation between air temperature and SVF in Singapore (*Wong and Jusuf, submitted*). The study concluded that during daytime, there is a strong correlation between air temperature and SVF. The higher SVF leads to a higher air temperature, which means there is no obstruction for solar radiation to heat up the environment. During nighttime, specifically at around 05.00-07.00 hours, a very weak correlation between air temperature and SVF was found, in line with the above-mentioned general theory. The findings supported the regression model results. The SVF in T_{avg} and T_{max} models have both positive signs in regression coefficient and Pearson correlation values. Furthermore, they are significant in

relation to air temperature conditions. While in T_{min} models, it has a positive sign in regression coefficient and a negative sign in Pearson correlation value.

In all of the models, the ALB variable shows a positive sign in the regression coefficient, which is against the general theory. However, in the T_{min} and T_{avg} models, the correlation values are negative, while it is positive in the T_{max} model. According to Taha, *et.al.* (1988), the range of natural environment albedo is narrower than the individual building material. The existence of greenery at most of the measurement points also leads to a less variation in the ALB variable. Furthermore, anthropogenic heat is believed to influence the result, since some of the areas, which have large pavement areas are under construction. During daytime, when maximum air temperature is reached, ground surfaces absorb heat and radiate it over time rather than reflect it immediately. Consequently, the ALB value behaves against the general theory, but it explains the phenomenon in this research (Giridharan, *et. al.*, 2008).

The next stage is to develop the air temperature prediction models that use only the significant variables ($p<0.05$). The variables that have opposite sign between regression coefficient and Pearson correlation have also been removed.

Hence, the air temperature prediction models can be written as follows:

T_{min} (^oC) = 4.061 + 0.839 Ref T_{min} (^oC) + 0.004 PAVE (%) – 0.193 GnPR – 0.029 HBDG + 1.339E-06 WALL (m^2)

R^2 = 0.86, F = 1707.45 and Std. Error = 0.47 (Sig. 0.00) (2)

T_{avg} (^oC) = 2.347 + 0.904 Ref T_{avg} (^oC) + 5.786E-05 $SOLAR_{total}$ (W/m^2) + 0.007 PAVE (%) – 0.06 GnPR – 0.015 HBDG + 1.311E-05 WALL (m^2) + 0.633 SVF

R^2 = 0.91, F = 2170.49 and Std. Error = 0.27 (Sig. 0.00) (3)

T_{max} (^oC) = 7.542 + 0.684 Ref T_{max} (^oC) + 0.003 $SOLAR_{max}$ (W/m^2) + 0.005 PAVE (%) – 0.016 HBDG + 6.777E-06 WALL (m^2) + 1.467 SVF + 1.466 ALB

R^2 = 0.54, F = 241.92 and Std. Error = 0.59 (Sig. 0.00) (4)

Models validation The air temperature regression models were developed based on the data of few years' periods. It is necessary to validate the models with another period of measurement data, which in this case, fairly clear and calm day conditions (wind speed <3m/s).

Figure 4. The comparison between measured and calculated minimum air temperature (T_{min}) and the box and whisker plot of the minimum air temperature difference between measured and calculated temperature

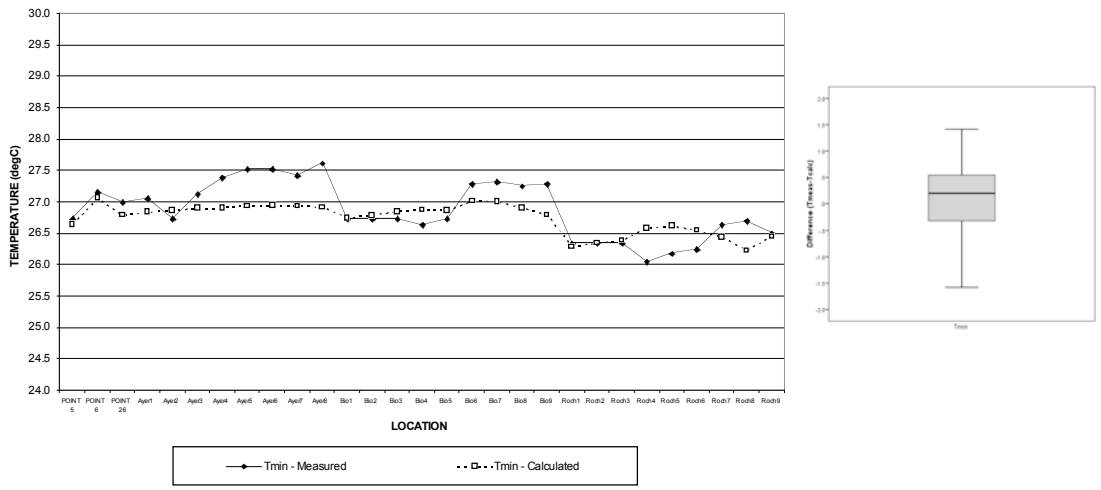

Figure 4 shows the validation of minimum air temperature model (T_{min}). It shows that the calculated minimum air temperature can fit with the measured one. From the box and whisker plot, it can be derived that 50% of the difference between the calculated and measured minimum air temperature is within acceptable range of -0.3°C – 0.5°C.

Figure 5. The comparison between measured and calculated average air temperature (T_{avg}) and the box and whisker plot of the average air temperature difference between measured and calculated temperature

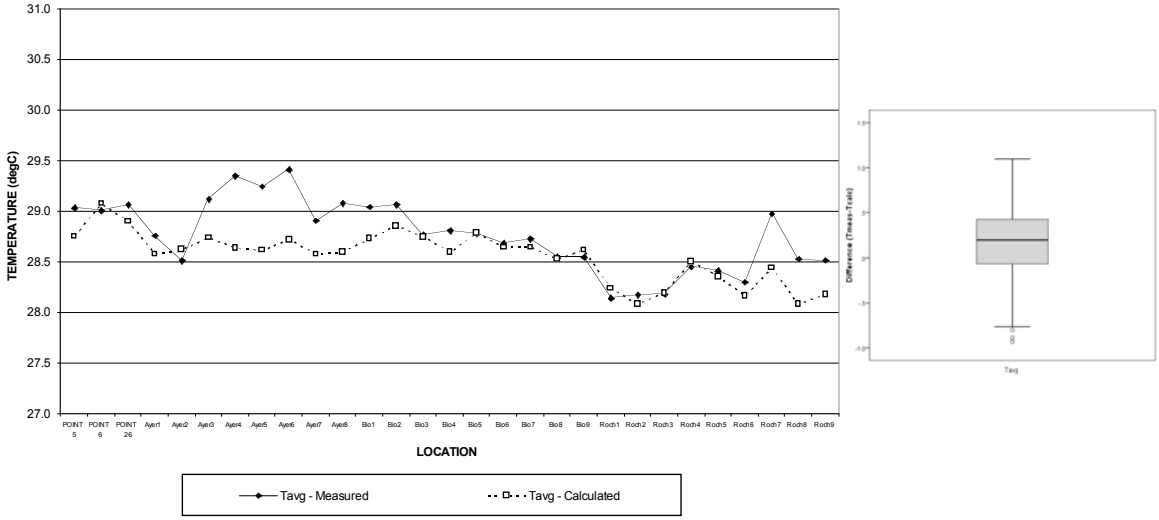

Figure 6. The comparison between measured and calculated maximum air temperature (T_{max}) and the box and whisker plot of the maximum air temperature difference between measured and calculated temperature

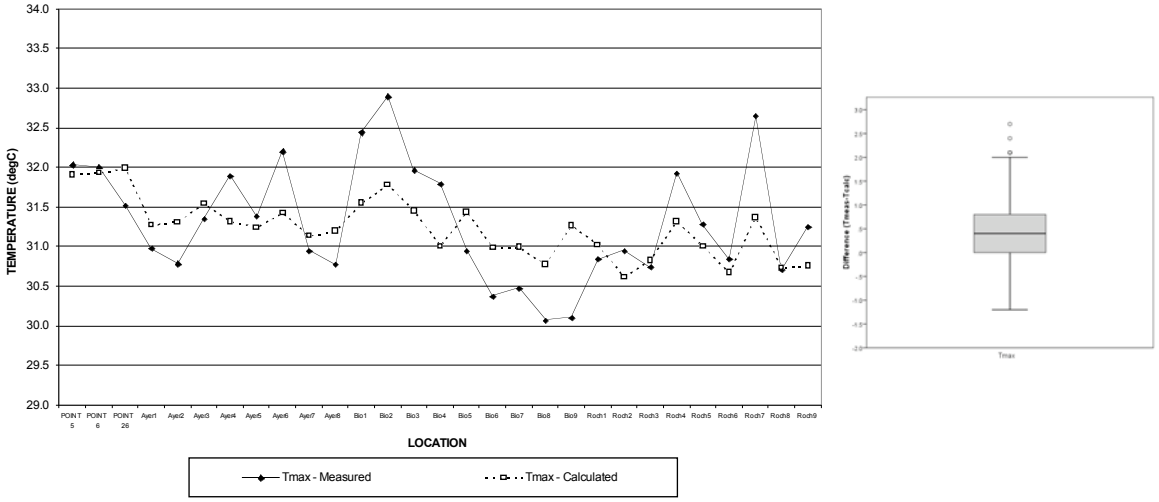

The validation of average air temperature models is shown in the Figure 5. Similar to the minimum air temperature model (T_{min}), the calculated result of average air temperature model (T_{avg}) is fit with the measured one. Observed from the box and whisker plot, 50% of the difference of measured and calculated average air temperature is between -0.1°C – 0.4°C.

Lastly, Figure 6 shows the validation for the maximum air temperature regression model (T_{max}). This model has fair R^2 value of 0.54. From the comparison graph, it can be observed that at some points, the difference of measured and calculated results is relatively large, more than 1^{o}C. It is believed that the existence of anthropogenic heat, which is not covered in the model, has the influence on the prediction model. On the other hand, as shown in the box and whisker plot, 50% of the difference the calculated and measured maximum air temperature is between 0^{o}C – 0.8^{o}C. Thus, although the difference is larger as compared to minimum and average temperature regression models, this model can still be used.

Sensitivity Analysis

The effect of the SVF reduction due to greenery varies the behavior of the predicted T_{min}, T_{avg} and T_{max} (see Figure 7). The increase of GnPR mainly governs the reduction of minimum air temperature, shown as a straight line. Meanwhile in the T_{avg} model, both GnPR and SVF influence the average temperature. When there is no greenery on site (GnPR = 0), the sky openness (SVF) is determined mainly by the canyon geometry. Greenery provides shading to the environment (reduces the SVF), thus, it reduces the air temperature. The reduction of average temperature is more prominent when GnPR is increased between 0-4 due to the combination factors of GnPR and SVF. Once the greenery completely covers up the openness to the sky, only the greenery density reduces the average air temperature, shown as a broken slope line. On the other hand, greenery density has indirect impact to the maximum air temperature. The increase of greenery density affects the openness to the sky, which reduces the maximum air temperature through its shading effect. Hence, as seen in Figure 7, when the trees have provided complete shading to the canyon at GnPR of 4, the increase of greenery density will have no further reduction in maximum air temperature.

Figure 7. Predicted T_{min}, T_{avg} and T_{max} for various values of GnPR

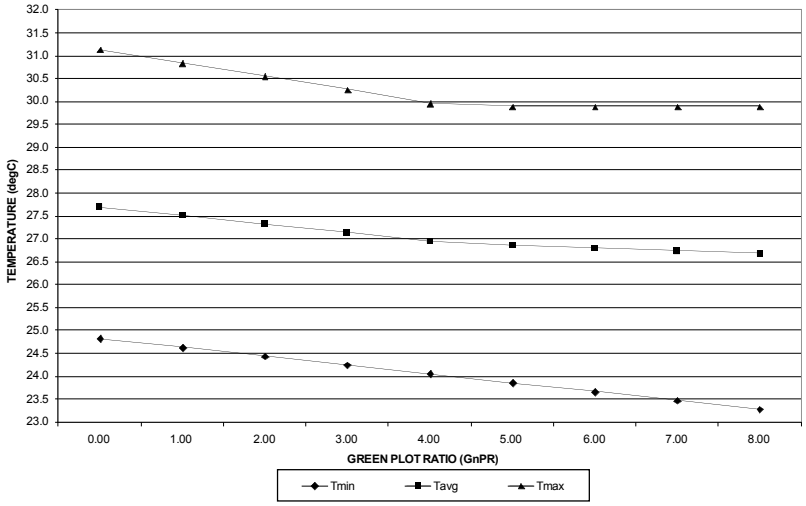

The change of building height seems to have relatively unnoticeable change on minimum air temperature, as shown in Figure 8a. The WALL area, together with the environment's thermal mass (HBDG), increases when the buildings get higher. A very small difference between the WALL and HDBG contributes to the reduction of minimum air temperature. The minimum air temperature reduction is still mainly influenced by greenery density (GnPR). The influence of building height on the predicted average air temperature is

clear (see Figure 8b). Looking at "V" profile in the graph where GnPR = 0, the average air temperature reduces when the building level is between 2 and 16. It shows that the increase of building height reduces the openness to the sky (SVF), i.e. provide shading. Once the canyon is completely shaded by the surrounding buildings, the further increase of building height, which further increases the WALL areas and shows the building density of the environment, starts having impact on the increase of the average air temperature. When the greenery density is increased, the turning point of graph (from reduced into increased average air temperature) is shifted towards the lower building heights, showing the relationship of GnPR in reducing SVF value.

The similar behavior has also appeared in the predicted maximum air temperature (see Figure 8c). However, since the greenery density has indirect relationship with the maximum air temperature through its relation with SVF, the reduction of maximum air temperature yields at GnPR = 5. Once the canyon is completely shaded, either due to buildings or due to greenery, the building density becomes the main contributor to the increase of maximum air temperature. The maximum air temperature is expected to remain at the same level when GnPR = 0 and number of storeys at 30, before it starts increasing when the building height is above 60 storeys.

Figure 8. Predicted T_{min} (a), T_{avg} (b) and T_{max} (c)for various values of No of storeys and GnPR

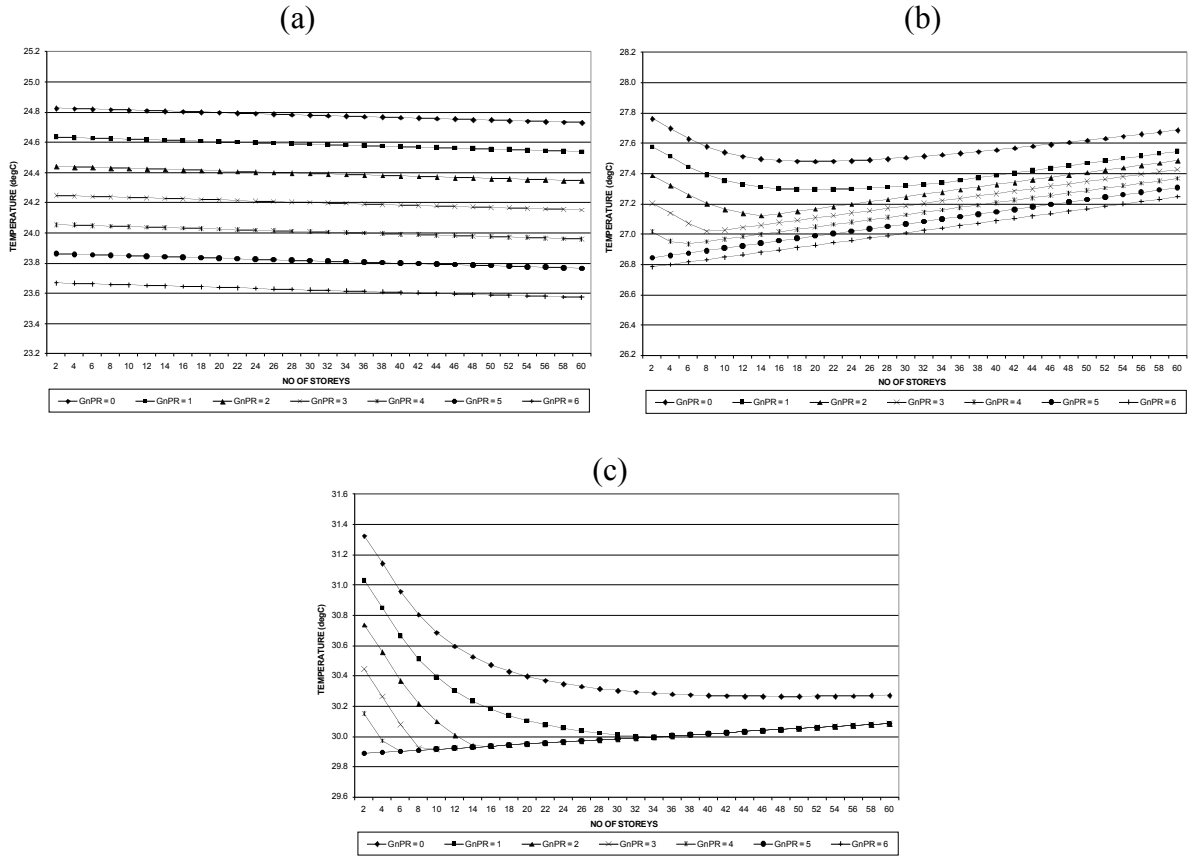

Figure 9 shows the predicted air temperature due to the increase of canyon width. In the T_{min} model, the increase of canyon width increases the pavement area (PAVE), which also increases the minimum air temperature, shown as an increasing trend when the canyon width is changed progressively from 15m to 45m. Meanwhile, in the T_{avg} and T_{max} models, the increase of average and maximum air temperatures is governed by the increase of PAVE and SVF values (see Figure 9a and 9b). At the same canyon width (e.g. at 15m), in the T_{avg}

model, the reduction of air temperature is governed by both GnPR and its impact on the reduction of SVF. When the greenery completely shades the canyon (SVF=0), only the greenery density (GnPR) reduces the air temperature. On the other hand, at the same canyon width in T_{max} model, once the SVF is 0, further increase on greenery density (GnPR) will not have any further reduction in maximum air temperature. Figure 9c shows the GnPR value yields at GnPR = 5.

Figure 9. Predicted T_{min} (a), T_{avg} (b) and T_{max} (c)for various values of canyon width and GnPR

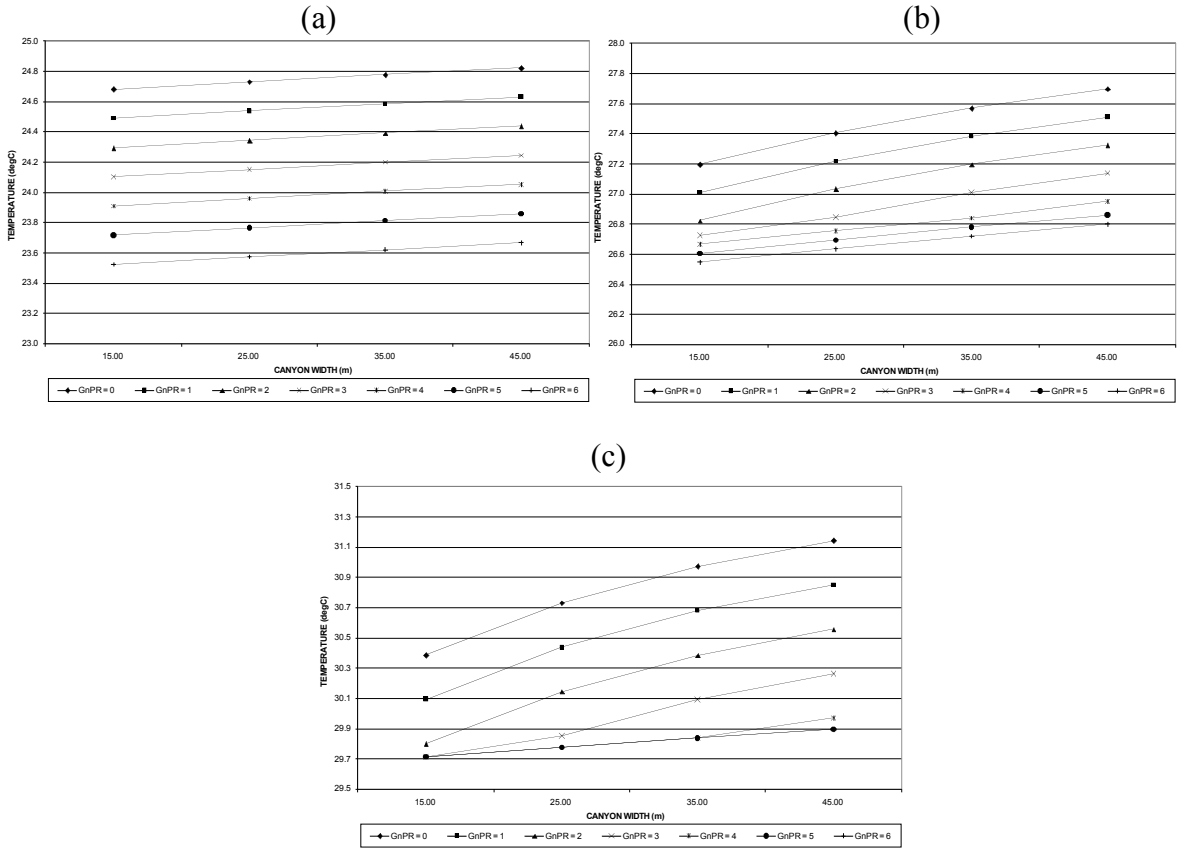

These sensitivity analyses have shown the relationships between some important urban planning variables. It is important for urban planners to find the optimum solutions between greenery, building characteristics and pavement distributions. Increasing the building height is not always having a negative impact (i.e. increase of air temperature). To a certain extent, it provides shading to the environment. On the other hand, widening the canyon width may have adverse impact during daytime, since it increases the openness to the sky, which increases the incoming solar radiation. In this situation, greenery has an important role in reducing the air temperature, through not only its evaporative cooling but also its shading. In these sensitivity analyses, the greenery density was calculated and limited only to the fixed greenery area and the density of trees. However, in the planning process, within the same radius of 50m, the greenery area can be increased, for example, by using vertical greenery and rooftop greening, since the concept Green Plot Ratio (GnPR) itself is three-dimensional.

Screening Tool for Estate Environment Evaluation (STEVE)

The Screening Tool for Estate Environment Evaluation (STEVE) was developed with a motivation as discussed above, to bridge research findings, especially air temperature prediction models, and urban planners. STEVE is a web-based application that is specific to an estate and it calculates the T_{min}, T_{avg} and T_{max} of a point of interest for the existing condition and future condition (proposed master plan) of an estate. The air temperature prediction models that have been discussed above were used in this application. In this version, STEVE was made for One-North estate (see Figure 10) and consists of three main interfaces: Estate's existing condition map, Estate's proposed master plan map and Calculator of air temperature predictions.

There are several steps involved in running STEVE, written as follows:

1. Select the estate condition: existing site or future development.
2. Select a point of location
3. Fill in the various variables listed in the Calculator page

Figure 10. STEVE main menus on first page

Existing Condition or Future Development Interface

The map of estate's existing condition or future development is displayed in this interface. The viewing level of the map is set into three levels. In level 1 (Figure 11a), it displays a complete estate map including the zoning boundaries, which are darkened when the mouse is pointed to the selected zone. Users are able to zoom-in the map into the second view level by clicking either the selected zone or the zoom-in button (Figure 11b). The designated points appear for the users' selection in this viewing level and then, users are able to predict air temperatures condition by clicking the selected point. A circle with the radius of 50 meters blinks to provide indication of urban morphology distribution that has the influence on air temperature at the selected point (Figure 11c).

Calculator Interface

At the left hand side of the existing or proposed master plan map, Calculator interface appears with preloaded values of different parameters for the selected point (Figure 12). The preloaded values can be changed according to users' need and the predicted air temperature results will appear with a push on the "Calculate" button.

The ***climatic predictors***, Ref T_{min}, Ref T_{avg}, Ref T_{max}, $SOLAR_{total}$ and $SOLAR_{max}$, can be obtained from either meteorological website or the available recorded data inside STEVE by clicking each predictor. The other ***urban morphology predictors***, PAVE, Average Building Height, BDG, WALL and ALB, are straightforward to be obtained. However, GnPR and SVF predictors are rather complicated. Hence, STEVE also provides GnPR and SVF calculators. A pop-up window will appear for the respective calculator by clicking each predictor.

Figure 11. First viewing level of the map (a), second viewing level of the map (b) and third viewing level of the map (c).

(a) (b)

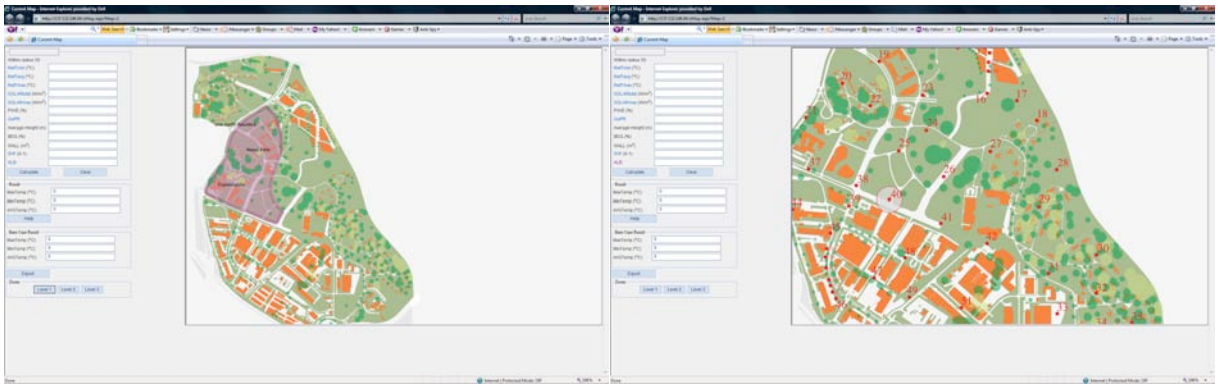

(c)

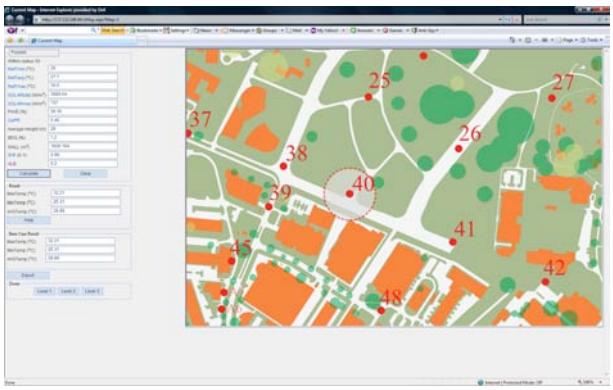

In GnPR calculator (Figure 13a), users need to specify up to a maximum of ten vegetation types, their quantities and their shade areas. The "Vegetation Type (LAI)" is the Leaf Area Index (LAI) values of the vegetations, which can be found in the shrubs and trees list. There are a total of 290 vegetation types inside the list. "Shade Area (m^2)" is actually the area of vegetation from its plan view. In the case of grass, both of "Vegetation Type (LAI) and "Nos. of vegetation" should be filled with a value of 1 while, "Shade Area (m^2)" is the area size of the grass itself. "Surface Area (m^2)" is the three-dimensional (3-D) area of a

circle with the radius of 50 meters when the area is not a flat land surface. Otherwise, it is simply a two-dimensional (2-D) circle area.

SVF calculator (Figure 13b) was developed based on the method by Oke (1981) and the corrected version of Steyn method (1980) by Barring (1985). Oke estimates the SVF by measuring the H/W ratio of the buildings with the assumption of ideal and infinitely long canyon geometry. Meanwhile, in Steyn's method, SVF obtained from fish-eye photographs is considered as the real SVF value than the Oke method, which was found underestimating the real SVF value. Barring further corrected the Steyn's method by regressing it with SVF by Oke's method as shown in eqn. 10.4.

The corresponding formulas for SVF calculator are written, as follows:

$$\theta = \tan^{-1}(H/(0.5W)) \quad (5)$$

$$SVF_{wall} = 0.5\ (\sin^2\theta + \cos\theta - 1)\ (\cos\theta)^{-1} \quad (6)$$

$$SVF_{sky} = (1 - 2\ SVF_{wall}) \quad (7)$$

$$SVF'_{steyn} = 0.033 + 1.004\ SVF_{sky} \quad (8)$$

In addition to the above corresponding formulas, the methodology of sensitivity analysis has discussed the relationship between SVF and GnPR that mainly due to trees. SVF value reduces by 0.2 for every increase of 1 GnPR. The variable of GnPR has also been included in the SVF calculator. However, users should remember that they should only fill in the GnPR variable, when only trees determine its value. Otherwise, the GnPR variable is 0.

Figure 12. Calculator interface

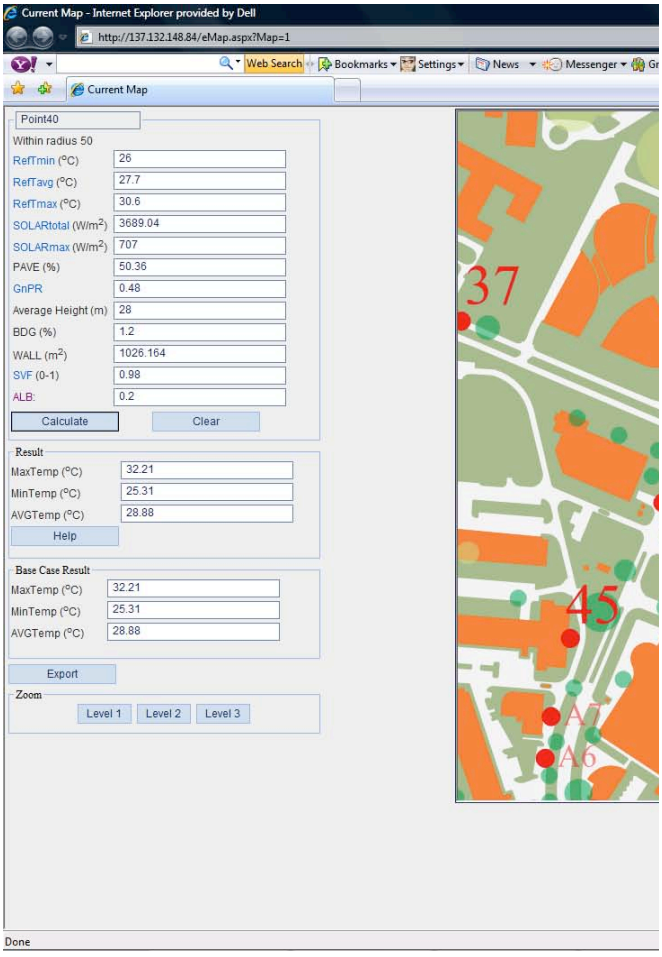

Figure 13. GnPR calculator (a) and SVF calculator (b)

(a) (b)

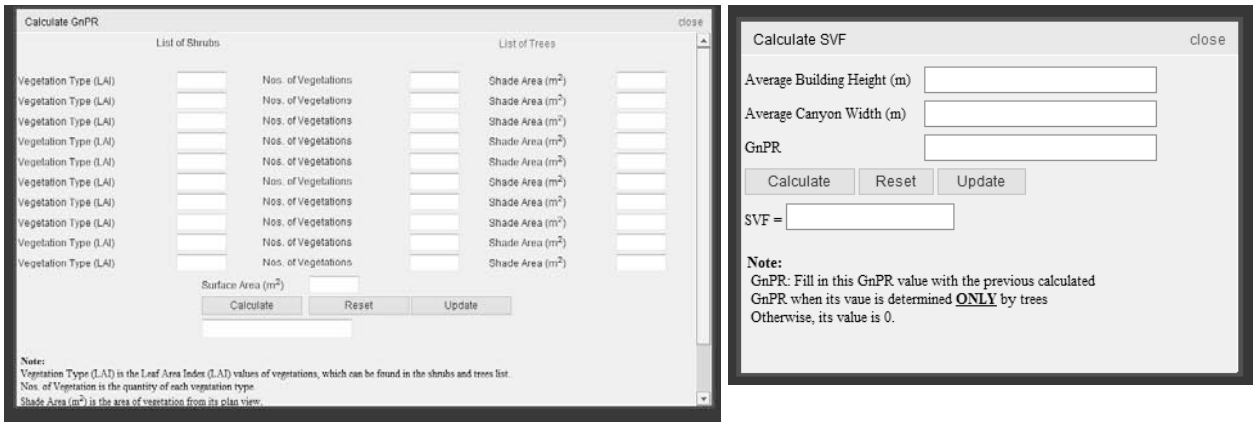

Conclusion

This paper has demonstrated the development of estate level empirical models of minimum (T_{min}), average (T_{avg}) and maximum (T_{max}) air temperature. In order to develop robust models, a long-term field measurement between September 2005 and March 2008 was carried out in two green Singapore estates, NUS and One-North. The field measurement had a total of 110 measurement points, which covered various land uses.

High R^2 values of 0.86 and 0.91 have been achieved for the T_{min} and T_{avg} models respectively. The comparison graphs between measured and calculated air temperature have shown a good fit and their differences are with the acceptable range. Meanwhile, T_{max} model has a fair R^2 value of 0.54. It is believed that anthropogenic heat, which was not covered in the model development, has influenced the result. However, box and whisker plot showed that the difference between measured and calculated is still acceptable.

The sensitivity analyses have also successfully shown the performance of the air temperature prediction models in relation to their variables. There is a close relationship between greenery, building characteristics and pavement distributions in influencing the air temperature conditions. Urban planners play an important role to minimize the negative impact to the environment as the result of their designs. It is important to learn that increasing building height is not always having a negative impact (i.e. increase of air temperature). It can be used to provide shading to the environment. On the other hand, increasing the canyon width may have adverse impact during daytime, since it increases the openness to the sky, which in turn increases the incoming solar radiation. In this situation, greenery has an important role in reducing air temperature, not only through its evaporative cooling but also through its shading. Therefore, urban planners should find the optimum design by adjusting the variables that meet the design objectives, including the economic objectives.

In urban climate modeling research, there is a gap between research findings and their usage by educated non-scientist. Many models are often too complicated and less user friendly for urban planners. Hence, it is necessary to develop a tool that bridges this gap.

STEVE is a web-based calculator of the air temperature prediction models that can be used to evaluate an estate's existing condition and to assess the proposed master plan for future development. It consists of three main interfaces: Estate's existing condition map, Estate's proposed master plan map and Calculator of air temperature predictions.

Limitation

The models development focused on fairly clear and calm (wind speed <3m/s) weather conditions. It is developed based on the climate condition of Singapore. Furthermore, anthropogenic heat release in the environment was not considered.
Some limitations of the first version of STEVE are written, as follows:

1. The existing condition and proposed master plan maps serve only as a guide map for the users or planners. Planners will not be able to change the master plan design inside STEVE platform. Design changes are done in different software, such as CAD software, calculate the new value of each urban morphology parameters and then, input them to STEVE calculator.
2. The locations of points were predetermined during STEVE development, working together with planners to select the representative points across the estate. For this reason, when planners would like to predict the air temperatures at other predetermined points, they need to get the value urban morphology parameters from CAD software and then input them to STEVE calculator.

References

Associated Press. (2007). *Singapore projects population will expand to 6.5 million in 40-50 years: cabinet minister*. Retrieved on 25th September 2008 from: http://www.iht.com/articles/ap/2007/02/27/asia/AS-GEN-Singapore-Population.php

Chapman, L., Thornes, J.E. and Bradley, A.V. (2001). Rapid determination of canyon geometry parameters for use in surface radiation budgets. *Theoretical and Applied Climatology*, 69, 81-89.

Department of Geography, NUS. (2008). *Geography Weather Station.* Retrieved on 6th April, 2008, from: http://courses.nus.edu.sg/course/geomr/front/fresearch/metstation/info01.htm

Eliasson, I. (1996). Urban nocturnal temperatures, street geometry and land use. *Atmospheric Environment,* 30, 379-392.

Giridharan, R., Lau, S.S.Y., Ganesan, S. and Givoni, B. (2007). Urban design factors influencing heat island intensity in high rise high density environments of Hong Kong. *Building and Environment*, 42, 3669-3684.

Giridharan, R., Lau, S.S.Y., Ganesan, S. and Givoni, B. (2008). Lowering the outdoor temperature in high-rise residential developments of coastal Hong Kong: the vegetation influence. *Building and Environment*, 43, 1583-1595.

ISO, 1975, *Standard atmosphere, ISO 2533:1975* (International Standard Organization).

Jusuf, S.K., Wong, N.H., Hagen, E., Anggoro, R. and Yan, H. (2007). The influence of land use on the urban heat island in Singapore. *Habitat International*, 31, 232-242.

Knowles, R.L. (1977). Energy and form: An ecological approach to urban growth. The MIT Press, USA.

Kruger, E. and Givoni, B. (2007). Outdoor measurements and temperature comparisons of seven monitoring stations: preliminary studies in Curitiba, Brazil. *Building and Environment,* 42, 1685-1698.

Laski, L. and Schellekens, S. (2007). Growing up urban. In Marshal, A. and Singer, A. (eds.), *The state of world population 2007 youth supplement*. United Nations Population Fund (UNFPA).

Matzarakis, A., Rutz, F., and Mayer, H. (2000). Estimation and calculation of the mean radiant temperature within urban structures. In: de Dear, R.J., Kalma, J.D., Oke, T.R. and Auliciems, A.(eds.). *Biometeorology and Urban Climatology at the Turn of the Millennium.* Selected Papers from the Conference ICB-ICUC'99, Sydney, WCASP-50, WMO/TD No. 1026, 273-278.

Oke, T.R. and Eas, C. (1971). The urban boundary layer in Montreal. *Boundary-Layer Meteorology*, 1, 411-437.

Oke, T.R. (1981). Canyon geometry and the nocturnal urban heat island: comparison of scale model and field observations. *International Journal of Climatology*, 1(1-4), 237-254.

Oke, T.R., Johnson, G.T., Steyn, D.G. and Watson, I.D. (1991). Simulation of surface urban heat islands under 'ideal' conditions at night. Part 2: Diagnosis of causation. *Boundary-Layer Meteorology*, 56, 339-358

Padmanabhamurty. (1990/91) Microclimates in tropical urban complexes. *Energy and Buildings*, 15 (3-4), 83-92.

Sani, S. (1990/91). Urban climatology in Malaysia: an overview. *Energy and Buildings*, 15 (3-4), 105-117.

Santamouris, M. (2001). The canyon effect. In: Santamouris, M. (editor). *Energy and climate in the urban built environment*. James & James Science Publishers, London.

Swaid, H. and Hoffman M.E. (1990). Prediction of urban air temperature variations using the analytical CTTC model. *Energy and Buildings*, 14, 313–324.

Taha, H., Akbari, H., Rosenfeld, A. and Huang, J. (1988). Residential cooling loads and the urban heat island-the effects of albedo. *Building and Environment*, 23(4), 271-283.

Wikipedia. (2008). *List of countries by population density*. Retrieved on 25th September 2008 from: http://en.wikipedia.org/wiki/List_of_countries_by_population_density

Wong, N.H. and Chen, Y. (2009). *Tropical urban heat islands: Climate, building and greenery*. Taylor and Francis, UK.

Wong, N.H., Jusuf, S.K. La Win, A.A., Htun, K.T., Negara, T.S. and Wu, X. (2007). Environmental study of the impact of greenery in an institutional campus in the tropics. *Building and environment*, 42, 2949–2970.

Wong, N.H. and Jusuf, S.K. Air temperature distribution and the influence of sky view factor on air temperature in a green Singapore estate. *Submitted to Journal of Urban Planning and Development.*